Available online at www.sciencedirect.com
SCIENCE DIRECT®
Thermochimica Acta 428 (2005) 173–183
thermochimica acta
www.elsevier.com/locate/tca

Some physico-chemical alterations caused by mechanochemical treatments in kaolinites of different structural order

Carmen Vizcayno[a,*], Ricardo Castelló[a], Irene Ranz[a], Benjamin Calvo[b]

[a] *Center for Environmental Sciences, CSIC, Serrano 115 dup, 28006 Madrid, Spain*
[b] *Department of Geological Engineering, School of Mining, University of Technology, Rios Rosas 21, 28003 Madrid, Spain*

Received 5 April 2004; received in revised form 29 October 2004; accepted 3 November 2004
Available online 13 December 2004

Abstract

Two kaolinites of different structural order designated KGa-2 and KC were milled for variable times (15, 30, 45, 60, 75, 90, 105 and 120 min). The ensuing changes were monitored using particle size distribution (PSD) analyses, pH measurements and thermal methods [thermogravimetric analysis (TGA), and differential thermal analysis (DTA)]. The size mode for the initial particles ranged from 0.31 to 0.36 μm in KGa-2 and from 6.6 to 7.7 μm in KC. After 120 min of milling, however, both kaolinites exhibited similar PSD results and modes (26.2–30.5 μm). Milling caused the transformation of surface charges and produced water molecules. This resulted in a decreased pH in KC and an increased one in KGa-2; however, both tended to converge on pH 6 after several minutes of milling. The new larger particles were formed by bonding between the new water molecules formed. Based on the temperature at which they disappeared, the water molecules were coordinated as zeolitic or interlayer water. The effects of milling became apparent at an earlier stage in the less ordered kaolinite. In well-ordered kaolinites consisting of large particles, the inner-to-inner surface hydroxyl ratio results in a symmetric dehydroxylation effect; thus, milling increased structural disorder and decreased the peak temperature, symmetry and width. Also, $T_p - T_{on}$ increased by effect of an increased presence of edges and inner surface hydroxyls, whereas $T_{off} - T_p$ decreased with decreasing proportion of inner hydroxyls relative to other types of OH groups.

Keywords: Kaolinite; Mechanochemical treatment; Thermal methods; Particle size distribution

1. Introduction

Kaolinite is one of the most abundant minerals in the Earth crust. Some of its properties (viz. colour, particle size, morphology, surface chemistry and charge) are exploited by the papermaking, paint and pharmaceutical industries, among others [1].

A number of techniques have been developed in recent years in order to alter the physical, chemical, structural and surface properties of kaolinite with a view to expanding or improving its applications. The treatments used to this end include (a) calcination at different temperatures [1]; (b) application of ionic and/or polar surfactants to turn its hydrophilicity into hydrophobicity or organophilicity [1]; (c) amorphization by milling [2]; (d) zeolitization by treatment with Na, Ca, Mg and K oxides at 100 °C [1]; (e) acidification [3]; (f) various combinations of the previous ones [4].

Milling an inorganic material causes the disintegration of particles and the consequent formation of new active surfaces in addition to changes in its physico-chemical properties that decrease its crystallinity (through amorphization) and increase it surface reactivity [5,6]. These "mechanochemical" effects are observed mainly when the material is milled using equipment involving friction and impaction forces on particles (e.g. vibratory, oscillating or planetary mills). Mechanochemical reactions can be classified into four broad categories [7], namely: (a) atom diffusion (prototropy), (b)

* Corresponding author. Tel.: +34 917452500; fax: +34 915640800.
E-mail addresses: cvizcayno@ccma.csic.es (C. Vizcayno), rcastello@ccma.csic.es (R. Castelló), irene.ranz@ccma.csic.es (I. Ranz), bcalvo@dinge.upm.es (B. Calvo).

0040-6031/$ – see front matter © 2004 Elsevier B.V. All rights reserved.
doi:10.1016/j.tca.2004.11.012

displacement between layers (delamination), (c) layer disruption and (d) adsorption of atmospheric water by the amorphous product.

The physical disintegration of kaolinite crystalline grains results in its gradual destruction via alterations in properties such as specific surface area, ion-exchange capacity, water absorption capacity and acid solubility, as well as through the formation of spherical aggregates of fine particles [2,8–15]. Changes in surface area with milling occur in three steps [14], namely: (a) the formation of new surfaces, (b) aggregation (viz. a monotonic decrease in the area change with milling time) and (c) agglomeration (which decreases the surface area).

The mechanochemical amorphization of kaolinite [11] involves layer disruption and grouping, rearrangement of coordinated polyhedra and proton transfer to other sites in the structure (an effect known as "prototropy" [16]); the result is an array of tetrahedral residual layers, and of octahedra and tetrahedra distorted to an extent dependent on the particle size and initial order [17], as well as on the particular milling method used.

Milling is highly likely to cause a large enough temperature change at a specific contact point for Al–OH and O–H bonds to be distorted or even broken, thereby leading to dehydroxylation and the formation of water molecules [14]. The water is formed by interaction of two hydroxyl groups in a two-step process: in the first, one hydroxyl group dissociates by proton transfer (prototropy) leaving a chemically bonded oxygen, as a superoxide anion, in the lattice; in the second, the proton released in the first step bonds to the other hydroxyl group to form a water molecule. If the process involves two adjacent OH groups, then it is *homogeneous*; otherwise, diffusion occurs and the water molecule is formed on the outer surface, the process being *heterogeneous* [18].

Despite the previous evidence, some aspects of the changes induced by milling in kaolinite are still obscure. Thus, the following questions remain unanswered: (a) do particle aggregates behave as a single particle or are they easily disintegrated? (b) why does reactivity increase with increasing particle size? The aim of this work was to acquire new information with a view to facilitating the interpretation of mechanochemical changes in kaolinite.

2. Material and methods

2.1. Material

The well-ordered kaolinite (KC) was supplied by Caosil (Guadalajara, Spain) with a Hinckley index of 1.19; the disordered kaolinite (KGa-2) was from Georgia (USA) and obtained from the Source Clay Repository of the Clay Minerals Society (MO, USA) with a Hinckley index of 0.43. Both were of sedimentary origin and the major mineral component was kaolinite (>95%) with a minor amount of quartz and mica in KC, and a small amount of anatase and mica in KGa-2.

The chemical composition, in wt.% as oxides, is SiO_2 45.82, Al_2O_3 37.65, Fe_2O_3 0.97, K_2O 0.80, loss on ignition 14.76 in KC; SiO_2 43.49, Al_2O_3 38.14, Fe_2O_3 1.15; TiO_2 1.91, K_2O 0.02, P_2O_5 0.32, loss on ignition 14.97 in KGa-2.

To study if the changes were due to the particle size or to structural modifications, the kaolinite from Georgia was separated into >20, 20–10, 10–5, 5–2 and 2–1 μm fractions by sedimentation, and into 1–0.5, 0.5–0.1 and <0.1 μm fractions by centrifugation.

2.2. Milling procedure

The solids were subjected to mechanical treatment in a Fritsch Pulverisette-7 planetary mill. Samples were milled for 15, 30, 45, 60, 75, 90, 105 or 120 min. In each test, an amount of 3 g of air-dried sample was milled in a 25 cm^3 stainless steel pot with the aid of three stainless steel balls; one ball was 15 mm in diameter and 13.6 g in weight, and the other two 12 mm in diameter and 7 g in weight. The rotation speed used was 730 rpm.

2.3. Particle size distribution

The particle size distribution (PSD) of the natural and milled samples was determined on a Malver Instruments Mastersizer-S instrument. Test was conducted in suspension. In order to avoid flocculation, samples were supplied with sodium polyphosphate (3.6%) and sodium carbonate (0.8%) as dispersants and ultrasonicated for 5 min. Then, in the compartment of small volume, the suspension was stirred at 3510 rpm and ultrasonicated. The lens used was 300 mm in focal length, so the measuring range was 0.05–900 μm. Each sample was analysed eight times.

2.4. pH measurements

The pH of the samples was measured with a Mettler 340 pH-meter following stirring of a 1:2.5 sample/de-ionized water suspension for 10 min and standing for 30 min.

2.5. Thermal methods

The thermal methods used (viz. TG, DTA and DTG) were implemented in a Setsys-16 instrument from Setaram, using 100 μl platinum crucibles, Pt/Pt10% Rh thermocouples, an argon stream at a flow-rate of 6.3 l/h, milled alumina as reference sample. Both the alumina and the samples were compacted in the absence of applied pressure. Prior to heating (at a rate of 10 °C/min), an isotherm was recorded at 25 °C for 1000 s.

The Setsoft 2000 module coupled to the thermal analyser allowed us to determine the mass change between two points in the TG curve or the areas of the peaks (by integration, using DTG and DTA). Also, the DTA curves gave the onset and offset points, which were bound by the intersect of the baseline with the tangent at the inflection point between the rising and falling segments (Fig. 1). Peak width was taken to

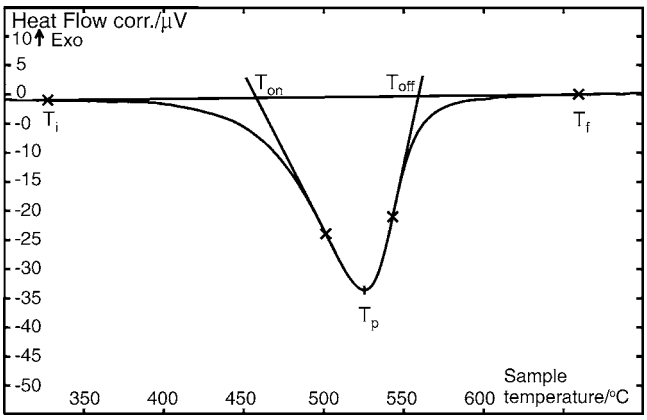

Fig. 1. Characteristic peak temperatures.

be the temperature difference between the offset (T_{off}) and onset (T_{on}) and the peak symmetry was calculated from the ratio $(T_p - T_{on})/(T_{off} - T_p)$.

Temperatures were standardized with SiO_2 alone, so the reported weight loss and heat flow were relative to the other samples.

3. Results

3.1. Particle size distribution

The results obtained in the PSD analysis of the natural kaolinites and milled samples are shown in Fig. 2 and classified into groups of particle sizes as close as possible to the fractionation ranges in Tables 1 and 2.

Milling the KC natural sample gave rise to four particle size ranges, namely: <2, 2–10, 10–20 and >20 μm. The proportion of particles in the <2, and 10–20 μm fractions changed little with the milling time. On the other hand, those of particles in 2–10 and >20 μm fractions decreased and increased, respectively, after 45 min of milling. Proportions levelled off after 75 min.

Based on the PSD results for the KGa-2 natural sample, most of its particles were very small (0.09–0.49 μm). The initial distribution was considerably altered after only 15 min of milling, but no substantial changes were observed beyond that point. The milled samples spanned three different size ranges, namely: <1, 1–20 and >20 μm. The proportion of particles in the first decreased after only 15 min of milling; that in the third exhibited the opposite trend and that in the second only very slight changes.

Both types of kaolinite had an identical mode (26.20–30.53 μm) and a similar particle size distribution upon milling for 120 min (see Fig. 2d and h).

3.2. pH

The two natural samples had a rather different pH; thus, KC was neutral-alkaline, whereas KGa-2 was acidic. Also, they exhibited opposing trends upon milling. Thus, the pH of KC decreased from 7.8 to 6.2, whereas that of KGa-2 increased from 3.6 to 5.3 (Fig. 3). Differences in the surface charges were produced by the effects of diffusion, delamination, disruption, and reorganization, by milling in relationship to the size and the degree of order–disorder of the kaolinite. In the order kaolinite decreased OH^- and/or increased H^+; the opposite occurred in the disorder. After a certain milling time (15 min for KGa-2 and 60 min for KC), the pH virtually levelled off.

3.3. Thermal methods

3.3.1. Weight losses in the natural and milled samples

The weight losses undergone by the natural and milled samples (as determined by TG), and the temperature at which

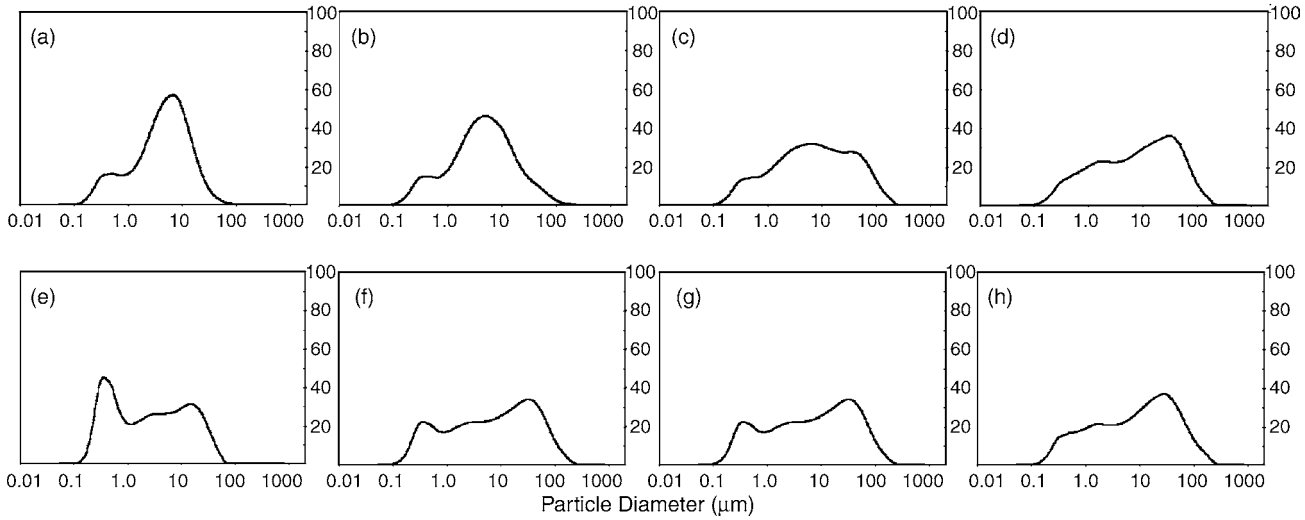

Fig. 2. Particle size distribution frequencies for the following samples: (a) natural KC, (b) KC milled for 30 min, (c) KC milled for 60 min, (d) KC milled for 120 min, (e) natural KGa-2, (f) KGa-2 milled for 15 min, (g) KGa-2 milled for 60 min and (h) KGa-2 milled for 120 min.

Table 1
Distribution of particle sizes (μm) in natural and milled KC

Size (μm)	Natural	15 min	30 min	45 min	60 min	75 min	90 min	120 min
<0.09	0.03	0.02	0.08	0.05	0.06	0.04	0.03	0.07
0.09–0.49	8.83	7.87	9.34	9.33	8.33	7.60	6.75	8.03
0.49–1.06	7.98	7.52	7.86	8.06	7.78	7.78	6.39	7.02
1.06–1.95	8.64	11.40	10.36	10.69	8.67	8.23	10.17	10.90
1.95–4.88	25.80	31.41	25.06	26.66	17.50	15.24	13.12	13.64
4.88–10.48	27.53	26.72	21.83	22.77	15.78	14.18	13.17	13.37
10.48–19.31	14.25	11.17	12.38	11.62	11.72	11.79	13.19	12.78
>19.31	6.97	3.89	13.09	10.82	30.16	35.14	37.18	34.19
D[4,3]	7.34	5.83	10.47	9.53	20.63	23.84	23.67	21.07
D[3,2]	1.62	1.65	1.51	1.51	1.74	1.90	2.04	1.76
$D(v,0.1)$	0.55	0.62	0.52	0.53	0.58	0.63	0.68	0.59
$D(v,0.5)$	4.72	3.94	4.47	4.21	7.06	8.92	10.68	8.95
$D(v,0.9)$	16.19	12.95	24.30	20.60	59.89	68.26	63.91	57.24
Mode	6.63–7.72	4.88–5.69	4.88–5.69	4.19–4.88	5.69–6.63	35.56–41.43	26.20–30.53	26.20–30.53

D[4,3] = mean diameter (on a volume basis) = $\sum d^4/\sum d^3$; D[3,2] = Sauter mean diameter (SMD) = $\sum d^3/\sum d^2$; $D(v,0.x)$ = percentiles (i.e. percentages below the size in question, on a volume basis); $D(v,0.5)$ (the 50 percentile) represents the median; mode = the most common value.

Table 2
Distribution of particle sizes (μm) in natural and milled KGa-2

Size (μm)	Natural	15 min	30 min	60 min	90 min	120 min
<0.09	0.01	0.04	0.04	0.05	0.03	0.03
0.09–0.49	23.14	12.99	10.51	8.96	8.46	8.73
0.49–1.06	14.39	7.39	6.60	7.72	8.21	7.01
1.06–1.95	8.68	9.42	9.11	7.17	7.71	10.20
1.95–4.88	15.37	13.24	12.62	11.77	12.31	12.68
4.88–10.48	13.63	11.89	11.92	12.13	12.72	12.54
10.48–19.31	12.25	11.32	11.88	12.74	13.48	12.89
>19.31	12.53	33.71	37.32	39.46	37.08	35.92
D[4,3]	7.40	21.15	22.74	26.41	23.26	23.26
D[3,2]	0.89	1.38	1.61	1.78	1.84	1.76
$D(v,0.1)$	0.31	0.40	0.47	0.54	0.57	0.55
$D(v,0.5)$	2.47	7.72	10.00	11.78	10.78	9.83
$D(v,0.9)$	22.06	59.33	61.85	66.28	60.33	62.64
Mode	0.31–0.36	30.53–35.56	30.53–35.56	30.53–35.56	26.20–30.53	26.20–30.53

D[4,3] = mean diameter (on a volume basis) = $\sum d^4/\sum d^3$; D[3,2] = Sauter mean diameter (SMD) = $\sum d^3/\sum d^2$; $D(v,0.x)$ = percentiles (i.e. percentages below the size in question, on a volume basis); $D(v,0.5)$ (the 50 percentile) represents the median; mode = the most common value.

Table 3
Percent weight loss (WL) and peak temperature (T_p) for natural and milled KC

Sample	25–95 °C		95–180 °C		180–380 °C	380–700 °C		700–1000 °C	95–1000 °C
	% WL	T_p	% WL	T_p	% WL	% WL	T_p	% WL	% WL
Natural	1.84	44.7	0.29	134.0	0.56	11.04	532.3	0.13	12.02
15 min	2.11	46.0	0.63	132.9	0.89	11.93	531.8	0.47	13.92
30 min	1.54	43.5	1.09	120.0	1.25	11.27	532.3	0.46	14.07
45 min	1.74	49.8	1.12	114.8	1.64	10.67	527.5	0.39	13.82
60 min	2.57	48.9	1.81	128.2	2.49	9.80	519.1	0.44	14.54
75 min	1.59	50.6	1.97	128.5	2.74	8.92	516.2	0.35	13.98
90 min	1.82	50.2	2.65	129.6	3.74	7.99	505.7	0.39	14.77
105 min	2.24	49.5	2.87	129.3	3.99	7.57	499.0	0.43	14.86
120 min	2.70	50.3	3.02	130.6	4.13	6.99	494.1	0.38	14.52

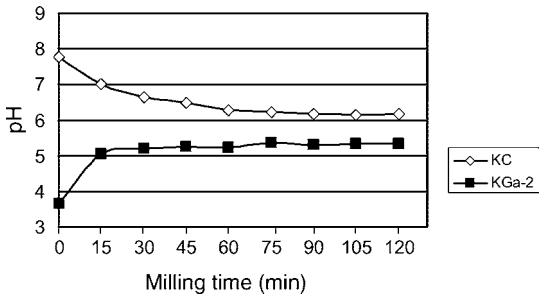

Fig. 3. Variation of pH with the milling time.

the dehydration and dehydroxylation peaks occurred (as determined by DTG) are listed in Tables 3 and 4.

Although the samples were held in a desiccator containing $CaCl_2$ for 24 h, and an isotherm was run at 25 °C for 1000 s, prior to each test, the weight losses between 25 and 95 °C exhibited no definite trend; this was a result of retained water being of the physisorbed type [19].

The weight loss between 95 and 180 °C in both kaolinites increased with increasing milling time through the formation of water molecules that were more strongly retained than physisorbed water. Weight losses over the range 180–380 °C also increased with increasing milling time; however, the absence of a DTG minimum (Figs. 4 and 5) suggests that the hydroxyl groups resulting from the mechanical rupture were bonded in a less uniform manner. On the other hand, weight losses over the range 380–700 °C decreased with increasing milling time as a result of the presence of fewer OH groups—part of the structure had already been destroyed and hydroxyl groups lost at lower temperatures.

3.3.2. Weight losses in the fractionated samples

The thermogravimetric study of the different fractions of natural KGa-2 (Table 5) revealed no changes (within experimental error) in weight losses among samples at temperatures up to 110 °C; only between 180 and 380 °C there was a slight increase with decreasing particle size associated to the amount of amorphous material present in such fractions observed. The <0.1 μm fraction exhibited dehydroxylation at higher temperatures, which is consistent with higher bonding energy.

These results lead to the conclusion that the weight losses are dependent to structural order–disorder but are independent to size particle.

3.3.3. Heat changes in the milled samples

3.3.3.1. Endothermal effect below 200 °C. All samples exhibited an endothermal effect peaking below 90 °C that was identical whichever the milling time. Between 120 and 130 °C, both types of kaolinites exhibited an additional endothermal effect that grew with increasing milling time. Because the two effects were overlapped, the heat changes involved could not be accurately determined; rather, they were examined separately by DTG.

3.3.3.2. Endothermal effect at ca. 500 °C. The temperature for the endothermal effect of the dehydroxylation of KC was slightly higher than that for KGa-2 (see Fig. 6a). Also, the peak temperature for the latter decreased from the beginning, whereas that for the former remained constant within the first 45 min and then decreased.

The amount of heat through dehydroxylation from both kaolinites was similar and decreased gradually with increasing milling time (Fig. 6b). If the heat flow values ($\mu V\ s\ mg^{-1}$) for the unmilled samples are taken to be 100%, then only 30% of the initial hydroxylation sites were preserved after 120 min of milling (Table 6).

The endothermal effect in the KC samples was more asymmetric. Also, its width decreased with increasing milling time by effect of the difference between T_{on} and T_p increasing by 10 °C; on the other hand, the difference between T_{off} and T_p decreased by nearly 20 °C upon milling for 120 min. By contrast, milling resulted in virtually no change in symmetry or peak width in KGa-2 (Fig. 7).

3.3.3.3. Exothermal effect at ca. 900 °C. The temperature of the exothermal peak was slightly higher for KC than for KGa-2 in both the natural and milled samples (Fig. 8); it decreased by 5 °C, with no symmetry change, after 120 min of milling. However, the amount of heat released by KGa-2 increased slightly with increasing milling, KC exhibiting the opposite trend.

Table 4
Percent weight loss (WL) and peak temperature (T_p) for natural and milled KGa-2

Sample	25–95 °C		95–180 °C		180–380 °C	380–700 °C		700–1000 °C	95–1000 °C
	% WL	T_p	% WL	T_p	% WL	% WL	T_p	% WL	% WL
Natural	1.85	45.4	0.32	135.0	0.81	15.12	526.2	0.37	16.62
15 min	2.71	45.9	1.00	125.6	1.70	12.61	516.1	0.51	15.82
30 min	2.44	49.7	1.25	136.0	1.93	11.15	509.1	0.29	14.62
45 min	3.05	48.1	1.83	127.2	2.60	10.78	509.3	0.40	15.61
60 min	2.80	48.9	2.18	128.8	3.09	9.91	504.1	0.34	15.52
75 min	3.57	48.8	2.71	128.1	3.80	9.26	497.0	0.50	16.27
90 min	3.26	49.3	2.90	128.9	4.11	8.68	495.2	0.44	16.13
105 min	2.76	49.5	2.91	131.9	4.06	7.65	487.4	0.28	14.90
120 min	2.99	49.3	3.26	130.3	4.51	7.39	485.5	0.42	15.58

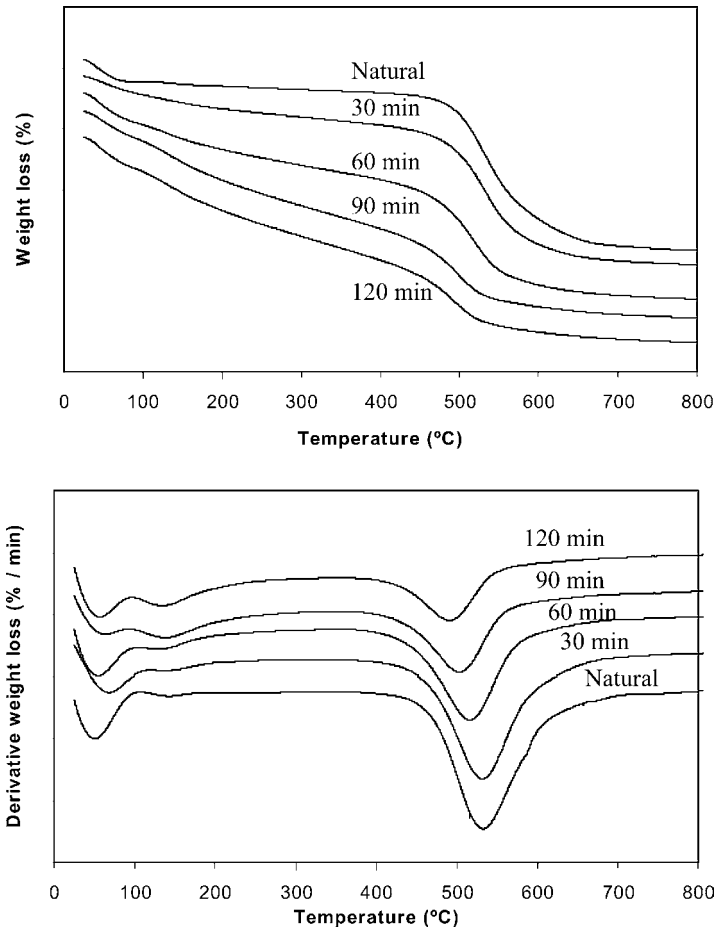

Fig. 4. TG and DTG curves for natural and milled KC.

3.3.4. Heat changes in the fractionated samples

3.3.4.1. Endothermal effect below 200 °C. The samples exhibited an endothermal effect at 58 °C; the temperature, however, decreased in the particle size >10 μm. One another very weak endothermal effect was observed between 134 and 152 °C the temperature of which increased with decreasing particle size (Table 5).

3.3.4.2. Endothermal dehydroxylation effect. The onset, peak and offset temperatures exhibited only slight differences among particle size fractions. The heat flow decreased slightly with decreasing particle size (Fig. 9). On the other hand, peak symmetry and width exhibited virtually no change at particle sizes above 2 μm, but decreased in smaller particles (Fig. 10).

3.3.4.3. Exothermal transformation effect. As can be seen from Figs. 9 and 10, the temperature, heat flow and width of the exothermal peak remained constant in all fractions; by exception, the symmetry for the <0.1 μm fraction decreased.

Table 5
Percent weight loss (WL) and peak temperature (T_p) for the different grain size fractions of KGa-2

Sample (μm)	25–110 °C		110–180 °C		180–380 °C	380–700°C		700–1000 °C	110–1000 °C
	% WL	T_p	% WL	T_p	% WL	% WL	T_p	% WL	% WL
>20	2.10	45.4	0.50	134.7	1.42	13.36	517.7	0.47	15.75
20–10	2.63	44.0	0.52	135.2	1.47	13.08	507.3	0.62	15.69
10–5	2.30	58.0	0.43	143.9	1.65	13.51	517.7	0.48	16.07
5–2	2.49	57.9	0.61	141.6	1.86	11.33	514.8	0.44	14.24
2–1	2.13	58.8	0.23	151.4	1.20	13.24	514.7	0.05	14.72
1–0.5	3.02	57.6	0.50	148.4	2.17	14.00	513.6	0.53	17.20
0.5–0.1	2.58	57.7	0.42	150.0	2.82	13.58	510.7	0.44	17.26
<0.1	1.63	58.2	0.26	152.1	1.68	13.30	525.0	0.32	15.56

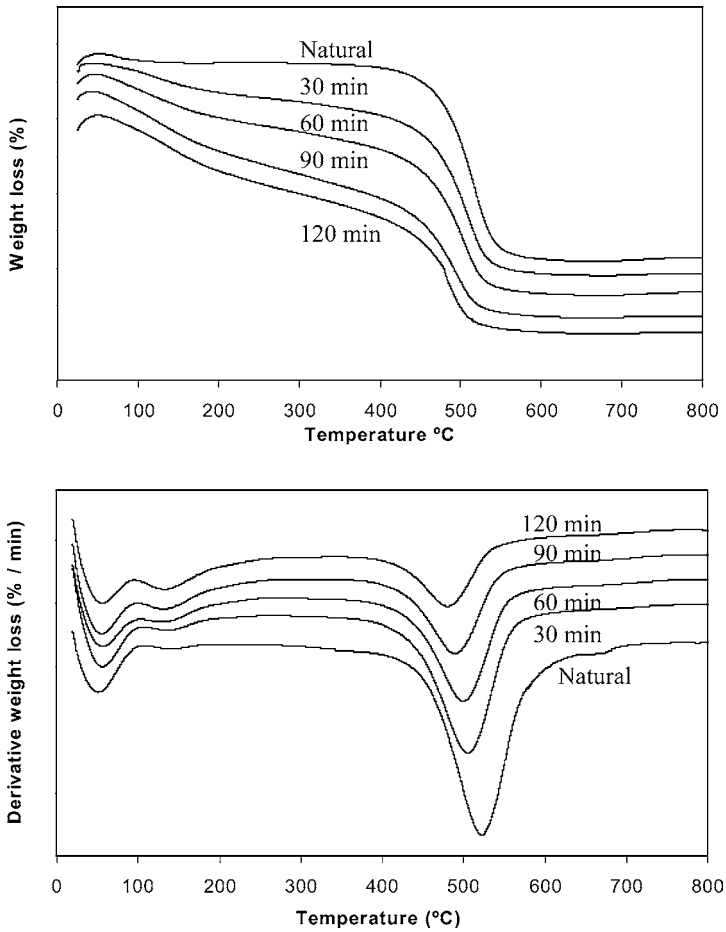

Fig. 5. TG and DTG curves for natural and milled KGa-2.

4. Discussion

The changes of the mode and mean diameter of the KC sample are consistent with the surface areas [2,9,14,17]. Initially, milling decreased particle size and that increased surface area. Subsequently, particles formed larger aggregates and reduced the surface area as a result. Finally, the aggregates formed clusters of constant size and area. Because the initial particle size in KGa-2 was so small (the mode was 0.3 μm), the first step observed in KC was absent here. As the aggregates could not be disintegrated by dispersants or ultrasounds, they can be assumed to behave as particles.

The layers in natural kaolinites possess three different types of surfaces, namely: (a) the plane of oxygen atoms bound to the Si tetrahedral layer; (b) the plane of hydroxyl groups bound to the Al octahedral layer; (c) the edges [20]. The layers are connected by hydrogen bonds [21,22] to form particles; therefore, the charge of a kaolinite particle depends on its diameter-to-thickness ratio [23]. The edges bear a different type of surface charge that is pH-dependent [21,24,25] and results from the cleavage of bonds on the periphery of the mineral; therefore, the charge increases with decreasing crystal size in kaolinite [26].

Milling breaks hydrogen bonds between layers and shifts them across the *ab* plane (delamination) forming particles with curved surfaces (27) similar to ones of halloysite; this action causes a decrease in the strength of the Si–O and Al–OH bonds at the edges. The MAS NMR technique [28] has revealed that the octahedral layers are more readily altered by milling than are the tetrahedral layers. Also, the FT-IR technique [14] has exposed the formation of water molecules and revealed that inner surface hydroxyls are lost before their inner counterparts. The broken hydrogen bonds between layers produced hydroxyl groups with different grades of acidity, which react to provide interlayer water by a homogeneous process [17,27]. On the other hand, the diminution in the strength bonds at the edges produced more activity and were able to form zeolitic water (heterogeneous process). The water molecules formed through milling (increased with milling time) were lost at 130 °C; this suggests that they were more strongly retained than physisorbed water molecules. The zeolitic or interlayer water from clay minerals [29], was lost at such temperature levels which is also similar in halloysites [30], and are assumed to be coordinated [17,18,27,30].

The fact that the weight loss increased with increasing milling time over the range 180–380 °C but decreased from

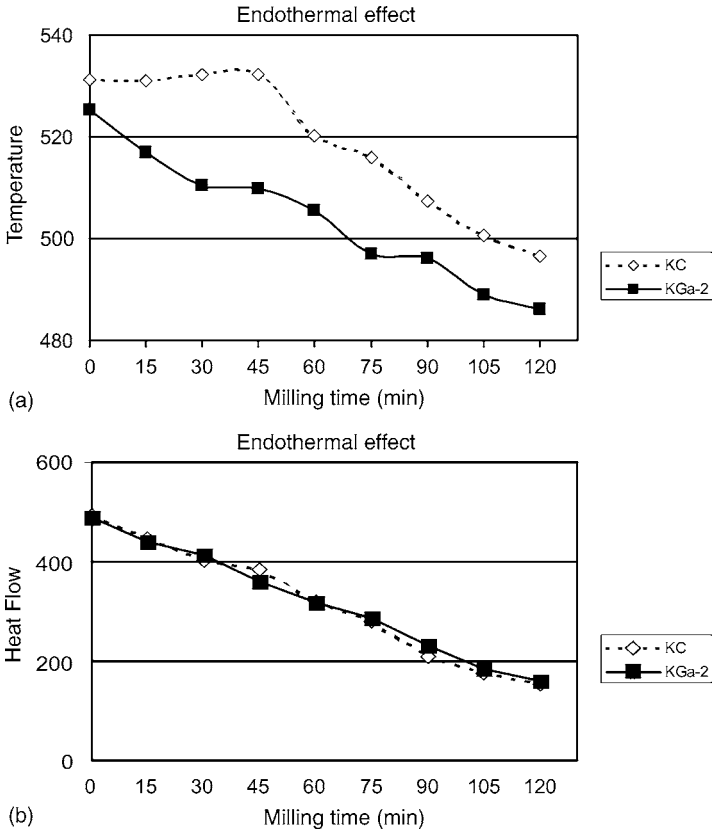

Fig. 6. Variation of the temperature (a) and heat flow (b) of the endothermal dehydroxylation effect with the milling time.

Table 6
Variation of the heat flow (%) of the endothermal effect at ca. 500 °C with the milling time

	Sample								
	Natural	15 min	30 min	45 min	60 min	75 min	90 min	105 min	120 min
KC	100	91	82	78	65	57	42	35	31
KGa-2	100	90	85	73	65	58	47	38	33

380 to 700 °C suggests that the hydroxyl groups are more weakly bound. The increased structural disorder resulting from the distortion of the tetrahedral and octahedral layers reduced the homogeneity of the hydroxyl groups, so they were more readily released. They were lost little by little without an inflexion point, and for this reason the peak is absent from the derivative recordings. However, some hydroxyl groups were still identified at positions similar to those in the initial sample (∼30%) – but more weakly bound as they were lost at a lower temperature – after 120 min of milling. The fact that the natural and milled samples exhibited similar weight loss changes between 95 and 1000 °C (within limit error) suggests that the water molecules were formed through internal transformations rather than via external processes [17].

In the KGa-2 sample, which possessed a smaller initial particle size (mode = 0.3 μm), the charge was located largely at the edges [25]. By virtue of its low pH (3.6), the protons were confronted with hydroxyl groups in the octahedral layer or the edges – which were loosened by milling – to form water molecules and raise the pH. In the KC sample, which possessed a larger particle size and a higher structural order, the high pH (7.8) relative to the previous one led to a prevalence of the charge of hydroxyl ions. If the charge originated from the plane of OH groups in the octahedral layer, then delayering would facilitate bonding to nearby protons in the same layer (*homogeneous* process) or protons at the edges (with an also decreased bonding energy). In the latter case, the process would be identical, albeit of opposite sign, for both kaolinites. On the other hand, if the negative charges in KC originated from the edges, bonds would be formed mainly between edges, thereby giving rise to larger particles and pores of a larger inner surface area. In any case, water molecules formed facilitate the connection between particles and the formation of larger ones.

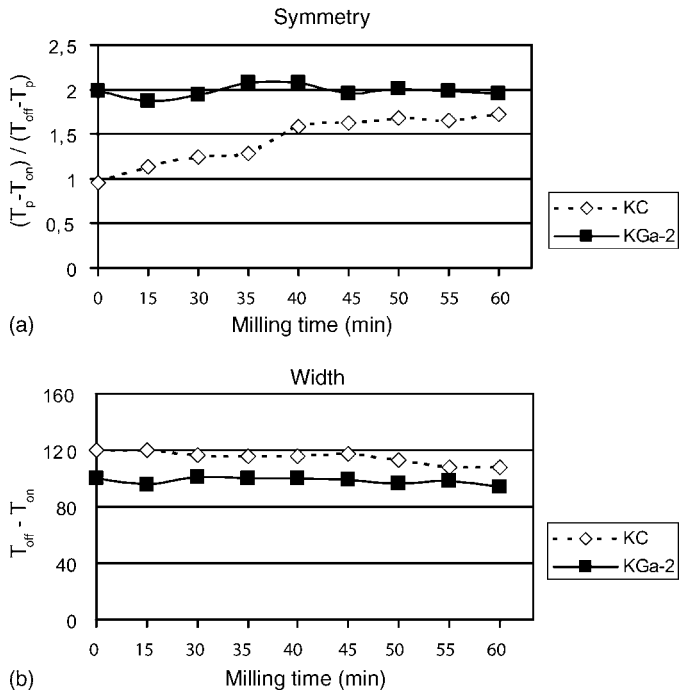

Fig. 7. Variation of the symmetry (a) and width (b) of the endothermal dehydroxylation peak with the milling time.

Some authors [17] have shown that the effectiveness of the mechanochemical treatment depends on the crystallinity of the kaolinite. However, in the samples KC and KGa-2, despite their rather different degrees of structural order and the particle sizes, exhibited a similar particle size distribution after milling for 120 min (Fig. 2d and h). Based on the heat flow results, roughly 67% of all releasable OH groups were modified by the milling (Table 6). As regards, the initial pH values for the two types of kaolinite were different; while that of KC was lowered and that of KGa-2 raised by milling, both levelled off at 6 (Fig. 3). Such effects, however, were appreciable only after 15 min of milling in the kaolinite with the lower structural order and particle size, and in the kaolinite with the higher initial structural order and particle size the effects of milling became apparent after 45 min.

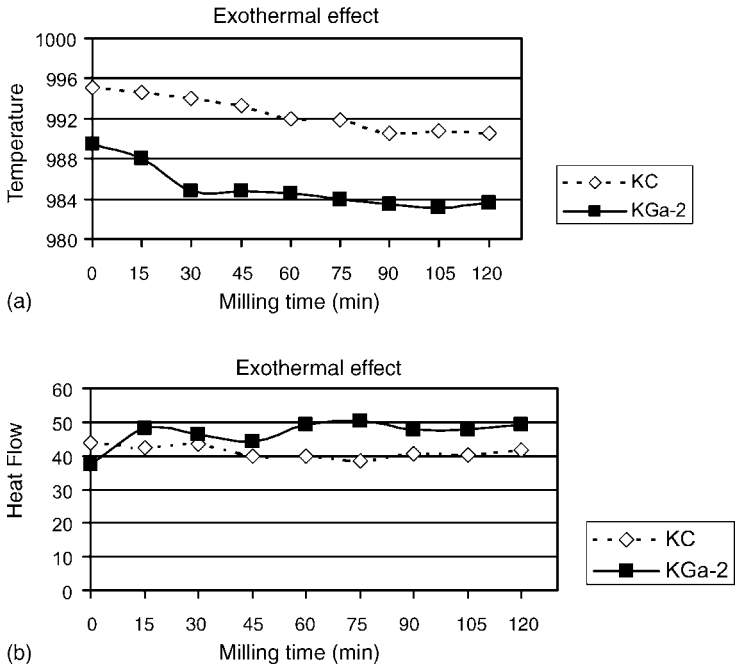

Fig. 8. Variation of the temperature (a) and heat flow (b) of the exothermal transformation effect with the milling time.

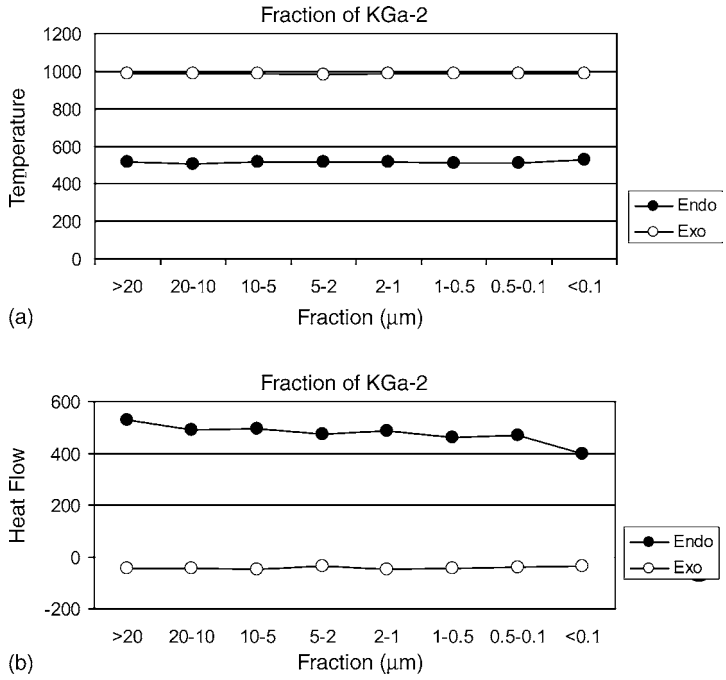

Fig. 9. Variation of the temperature (a) and heat flow (b) of the endothermal and exothermal effects in the different grain size fractions of KGa-2.

The endothermal dehydroxylation effect in the different grain-size fraction samples of KGa-2 were asymmetrical. $T_p - T_{on}$ was almost twice greater than $T_{off} - T_p$ (Fig. 10a). None of the temperatures (T_p, T_{on} or T_{off}) changed in the >1 μm fractions, only in the <1 μm fractions T_{off} decreased. This decreased of heat flow, peak width and symmetry was possibly because the small particle size favoured the presence of outer and inner surface hydroxyls over that of inner hydroxyls and the latter contributed to a greater extent to $T_{off} - T_p$.

In the natural KC sample, the endothermal dehydroxylation effect was symmetrical and 120 °C wide (Fig. 7). Milling decreased its peak area, symmetry and width—the latter is seemingly abnormal as the width should have increased

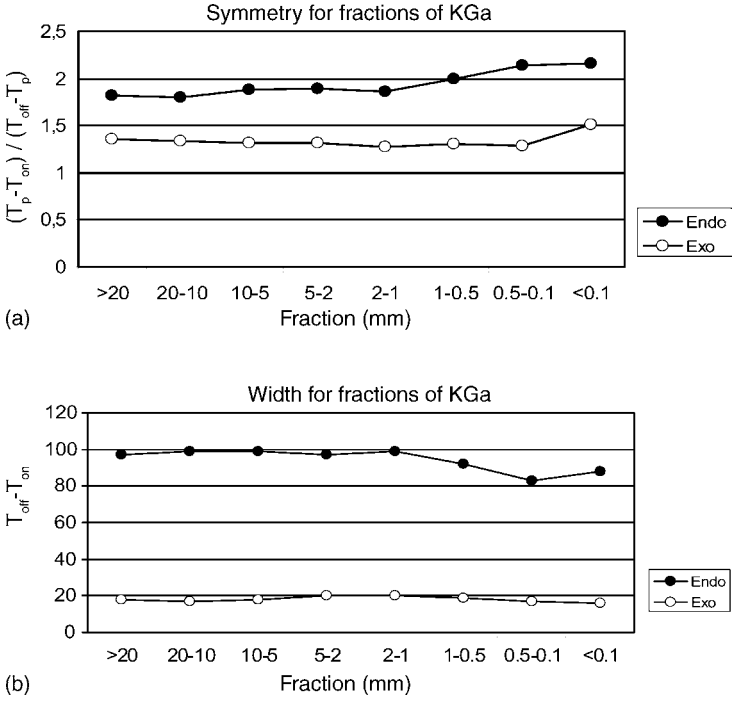

Fig. 10. Variation of the symmetry (a) and width (b) of the endothermal and exothermal effects in the different grain size fractions of KGa-2.

with increasing structural disorder. The peak area decreased because some hydroxyl groups were lost—after 120 min milling, only 31% remained. The inner-to-inner surface OH ratio in well-ordered kaolinites of a large particle size results in a symmetric dehydroxylation effect; milling increases structural disorder and decreases the peak temperature, increases $T_p - T_{on}$ by effect of increased OH groups at the edges and inner surfaces, and decreases $T_{off} - T_p$ through a decreased proportion of inner OH groups with respect to the other types of hydroxyls. However, in natural and milled samples of disordered kaolinite (KGa-2), there are no changes in symmetry or width. These results are in agreement with those obtained by FT-IR technique [27] revealed that the inner surface hydroxyls were lost before the inner hydroxyls in an ordered kaolinite, whereas in a disordered kaolinite they were lost simultaneously.

5. Conclusions

Milling two kaolinites of different structural order and particle size for variable times was found to result in a new structural ordering that led to larger particles. The new particles were made by bonds involving the new water molecules formed. Based on the temperature at which it was lost, such water molecules must be coordinated as zeolitic or interlayer water types.

The effects of milling became apparent after 45 min in KC, which was the kaolinite with the higher initial structural order and particle size. Such effects, however, were appreciable after only 15 min of milling in KGa-2, which was the kaolinite with the lower structural order and particle size.

Milling altered the pH of both kaolinites. Although natural KC is slightly alkaline and KGa-2 acidic, both converged on pH 6 upon milling.

In well-order kaolinites of a large particle size, the ratio of inner-to-inner surface hydroxyls results in a symmetric dehydroxylation effect. Milling increases structural disorder and decreases the peak temperature, symmetry and width; also, $T_p - T_{on}$ increases through an increased proportion of OH groups at the edges and inner surfaces, whereas $T_{off} - T_p$ decreases through a decreased proportion of inner hydroxyls relative to the other types of OH groups.

Acknowledgements

The authors thank Ms. M.J. Villoslada for performing the particle size distribution analyses. We gratefully acknowledge the valuable suggestions of the Prof. Vyazovkin and referees.

References

[1] H.H. Murray, Clay Miner. 34 (1999) 39–49.
[2] E.F. Aglietti, J.M. Porto López, E. Pereira, Int. J. Miner. Proc. 16 (1986) 125–133.
[3] T. Vengris, R. Binkiene, A. Sveikauskaite, Appl. Clay Sci. 18 (2001) 183–190.
[4] G. Suraj, C.S.P. Iyer, M. Lalithambika, Appl. Clay Sci. 13 (1998) 293–306.
[5] I.J. Lin, S. Naviv, D.J.M. Grodzian, Mater. Sci. Eng. 39 (1979) 193–209.
[6] J.M. Criado, M. González, M. Macias, Thermochim. Acta 135 (1988) 219–223.
[7] S. Yariv, I. Lapides, J. Mater. Syn. Proc. 8 (2000) 223–233.
[8] J.L. Perez-Rodriguez, L. Madrid Sánchez del Villar, P.J. Sánchez-Soto, Clay Miner. 23 (1988) 399–410.
[9] F. González García, M.T. Ruiz Abrio, M. Gonzalez Rodriguez, Clay Miner. 26 (1991) 549–565.
[10] P.J. Sanchez-Soto, M. Macias, J.L. Perez-Rodriguez, J. Am. Ceram. Soc. 76 (1993) 180–184.
[11] E. Kristof, A.Z. Juhasz, I. Vassányi, Clay Clay Miner. 41 (1993) 608–612.
[12] P.J. Sanchez Soto, A. Wiewiora, M.A. Avilés, A. Justo, L.A. Perez Maqueda, J.L. Perez-Rodriguez, P. Bylina, Appl. Clay Sci. 12 (1997) 297–312.
[13] R.L. Frost, E. Makó, J. Kristóf, E. Horváth, J.T. Kloprogge, J. Colloid Interface Sci. 239 (2001) 458–466.
[14] E. Makó, R.L. Frost, J. Kristóf, E. Horváth, J. Colloid Interface Sci. 244 (2001) 359–364.
[15] E.T. Stepkowska, J.L. Perez-Rodriguez, M.C. Jimenez de Haro, P.J. Sanchez Soto, C. Maqueda, Clay Miner. 36 (2001) 105–114.
[16] J.G. Miller, T.D. Outon, Clay Clay Miner. 18 (1970) 313–323.
[17] R.L. Frost, E. Horvath, E. Mako, J. Kristof, J. Colloid Interface Sci. 270 (2004) 337–346.
[18] R.L. Frost, E. Horváth, E. Makó, J. Kristóf, A. Redey, Thermochim. Acta 408 (2003) 103–113.
[19] N. Benharrants, M. Belbachir, A.P. Legrand, J.B. d'Espinose de la Caillerie, Clay Miner. 38 (2003) 49–61.
[20] K.M. Sparks, J.D. Wells, B.B. Johnson, Eur. J. Soil Sci. 46 (1995) 621–631.
[21] H.L. Bohn, B.L. McNeal, G.A. O'Connor, Soil Chemistry, 2nd ed., Wiley, New York, 1985.
[22] G. Sposito, The Chemistry of Soils, Oxford University Press, New York, 1989.
[23] W.B. Jepson, Philos. Trans. R. Soc., London Ser. A 311 (1984) 411–432.
[24] R.N. Yong, A.M.O. Mohaned, B.P. Warkentin, Principles of Contaminant Transport in Soils, Elsevier, New York, 1992.
[25] J.K. Mitchell, Fundamentals of Soil Behaviour, Wiley, New York, 1993.
[26] C. Ma, R.A. Eggleton, Clay Clay Miner. 47 (1999) 174–180.
[27] R.L. Frost, E. Horvath, E. Mako, J. Kristof, J. Colloid Interface Sci. 270 (2003) 386–395.
[28] J. Temuujin, K.J.D. Mackenzie, M. Schmucker, H. Schneider, J. McManus, S. Wimperis, J. Eur. Ceram. Soc. 20 (2001) 413–421.
[29] B. Velde, Introduction to Clay Mineral, Chapman & Hall, London, 1992.
[30] E. Horvath, R.L. Frost, E. Mako, J. Kristof, T. Cseh, Thermochim. Acta 404 (2003) 227–234.